Photosynthesis Research (2024) 159:291–301
https://doi.org/10.1007/s11120-023-01070-6

RESEARCH

Photogeneration and quenching of singlet molecular oxygen by bacterial C_{40} carotenoids with long chain of conjugated double bonds

A. S. Benditkis[1] · A. A. Ashikhmin[2] · A. A. Moskalenko[2] · A. A. Krasnovsky Jr.[1]

Received: 12 June 2023 / Accepted: 14 December 2023 / Published online: 5 February 2024

Abstract

Measurement of photosensitized luminescence of singlet oxygen has been applied to studies of singlet oxygen generation and quenching by C_{40} carotenoids (neurosporene, lycopene, rhodopin, and spirilloxanthin) with long chain of conjugated double bonds (CDB) using hexafluorobenzene as a solvent. It has been found that neurosporene, lycopene, and rhodopin are capable of the low efficient singlet oxygen generation in aerated solutions upon photoexcitation in the spectral region of their main absorption maxima. The quantum yield of this process was estimated to be $(1.5–3.0)\times10^{-2}$. This value is near the singlet oxygen yields in solutions of ζ-carotene (7 CDB) and phytoene (3 CDB) and many-fold smaller than in solutions of phytofluene (5 CDB) (Ashikhmin et al. Biochemistry (Mosc) 85:773–780, https://doi.org/10.1134/S0006297920070056, 2020, Biochemistry (Mosc) 87:1169–1178, 2022, https://doi.org/10.1134/S0006297922100108 2022). Photogeneration of singlet oxygen was not observed in spirilloxanthin solutions. A correlation was found between the singlet oxygen yields and the quantum yields and lifetimes of the fluorescence of the carotenoid molecules. All carotenoids were shown to be strong physical quenchers of singlet oxygen. The rate constants of $^1O_2$ quenching by the carotenoids with long chain of CDB (9–13) were close to the rate constant of the diffusion-limited reactions $\approx10^{10}$ M^{-1} s^{-1}, being many-fold greater than the rate constants of $^1O_2$ quenching by the carotenoids with the short chain of CDB (3–7) phytoene, phytofluene, and ζ-carotene studied in prior papers of our group (Ashikhmin et al. 2020, 2022). To our knowledge, the quenching rate constants of rhodopin and spirilloxanthin have been obtained in this paper for the first time. The mechanisms of $^1O_2$ photogeneration by carotenoids in solution and in the LH2 complexes of photosynthetic cells, as well as the efficiencies of their protective action are discussed.

Keywords Neurosporene · Rhodopin · Lycopene · Spirilloxanthin · Singlet oxygen · Photosensitization · Quenching · Light-harvesting complex

Abbreviations

BChl Bacteriochlorophyll a
CDB Conjugated double bonds

Introduction

Photosynthetic organisms often work under strong light stress when the intensity of incident light exceeds the ability of the photosynthetic cells to utilize light energy for photosynthesis. Protection from the photodynamic damage caused by excess light energy is a prerequisite of survival and normal functioning of the photosynthetic apparatus. After the pioneering work by Griffiths et al. (1955) and subsequent papers of other groups, it is generally adopted that carotenoids with nine and more conjugated double bonds (CDB) play an important role in protection of living tissues against photooxidative stress (Griffiths et al. 1955; Mathews-Roth et al. 1974; Foote 1976; Cogdell et al. 2000; Britton 2008 and refs therein). Contrary to this opinion, A. A. Moskalenko's Lab (Institute of Basic Biological Problems, Russia) obtained the data, which suggested that carotenoids photosensitize the $^1O_2$-mediated destruction

✉ A. A. Krasnovsky Jr.
phoal@mail.ru

[1] A.N. Bach Institute of Biochemistry, Federal Research Center of Biotechnology of the Russian Academy of Sciences, 119071 Moscow, Russia

[2] Pushchino Scientific Center for Biological Research of Russian Academy of Sciences, Institute of Basic Biological Problems, Russian Academy of Sciences, 142290 Pushchino, Russia

of bacteriochlorophyll (BChl) in the LH2 complexes of purple bacteria (Makhneva et al. 2007, 2009, 2020, 2021). As shown quite recently, the action spectrum of this process corresponds to the absorption spectra of rhodopin and lycopene. However, the quantum yield of the BChl photodestruction is very low, equal to 0.0003 (Klenina et al. 2022). Based on these observations, one could assume that carotenoids are capable of low efficient generation of singlet oxygen under photoexcitation in the bacterial photosynthetic apparatus. Perhaps, this process because of its low efficiency is not very important for photodamage of bacterial cells. However, we feel that it is of great interest from the viewpoint of photophysics of carotenoid molecules. It is noteworthy, that before our studies, photogeneration of $^1O_2$ by isolated molecules of bacterial carotenoids had never been investigated, although it is known that $^1O_2$ formation is rather efficiently photosensitized by the visual pigment—retinal, a polyene with 6 CDB (Delmelle 1979; Krasnovsky and Kagan 1979; Edge and Truscott 2018).

In this connection, couple of years ago, we have started a systematic study of $^1O_2$ photosensitization by bacterial carotenoids with different lengths of CDB using direct detection of carotenoid-photosensitized $^1O_2$ phosphorescence. It should be noted that photosensitized phosphorescence of singlet oxygen at 1270 nm in aerated solutions of different pigments, including chlorophylls, BChls and retinals, was firstly observed by one of us in nineteen seventies (Krasnovsky 1976, Krasnovskiĭ 1977; Krasnovsky 1979; Krasnovsky and Kagan 1979). Presently, detection of this phosphorescence is used worldwide as the most accurate method of singlet oxygen detection and investigation. The most common phosphorescence mechanism corresponds to the following scheme:

$$^1P_0 + h\nu \rightarrow {}^1P^* \rightarrow {}^3P^* + {}^3O_2 \rightarrow {}^1O_2$$
$$^1O_2 \rightarrow {}^3O_2 + h\nu\ (1270\ \text{nm}),$$

where $^1P_0$, $^1P^*$, and $^3P^*$ are molecules of a pigment-photosensitizer in the ground and excited singlet and triplet states, $^1O_2$ is the $^1\Delta_g$ singlet state of molecular oxygen (Krasnovsky 1979, 2008; Schweitzer and Schmidt 2003 and refs therein).

For our work, new $^1O_2$ phosphorescence spectrometers assembled recently by A.A. Krasnovsky's group (Bach Institute of Biochemistry, Russia) (Krasnovsky et al. 2019) were applied. In the previous papers, polyenes with a short chain of CDB were studied: phytoene (3 CDB), phytofluene (5 CDB), and ζ-carotene (7 CDB) (Ashikhmin et al. 2020, 2022). It was found that photoexcitation of these polyenes causes generation of $^1O_2$ in aerated solutions. The quantum yields of $^1O_2$ generation by phytoene and ζ-carotene appeared to be low: ≈ 0.02 and 0.014, respectively. Unexpectedly, phytofluene efficiently generated $^1O_2$. First estimation of the quantum yield (Φ_Δ) of this process based on the steady-state phosphorescence measurements led us to a value of 0.85 ± 0.05 (Ashikhmin et al. 2020). In the next paper, using more accurate time-resolved measurements, we arrived to a slightly lower value 0.39 ± 0.06, which is still very high (Ashikhmin et al. 2022). The rate constants of $^1O_2$ quenching by these carotenoids were also obtained (Ashikhmin et al. 2020, 2022). In the present work, the methods developed in the prior papers are applied to natural bacterial carotenoids with long chain of CDB: neurosporene (9 CDB), lycopene (11 CDB), rhodopin (11 CDB), and spirilloxanthin (13 CDB) (Fig. 1).

Materials and methods

Carotenoid isolation

Carotenoids were obtained from cells of purple photosynthetic bacteria. Neurosporene was isolated from *Rhodobacter sphaeroides* strain G1C (received from Prof. Takaichi S., Nippon Medical School, Japan). Lycopene was purified from *Ectothiorhodospira haloalkaliphila*. Rhodopin and spirilloxanthin were extracted from *Allochromatium vinosum* and *Rhodospirillum rubrum*, respectively. The bacterial cells used for carotenoid isolation were grown at 28 ± 2 °C in anaerobic conditions under illumination by white light of an incandescent lamp 90 W/m^2 on the Hutner's, Pfennig's,

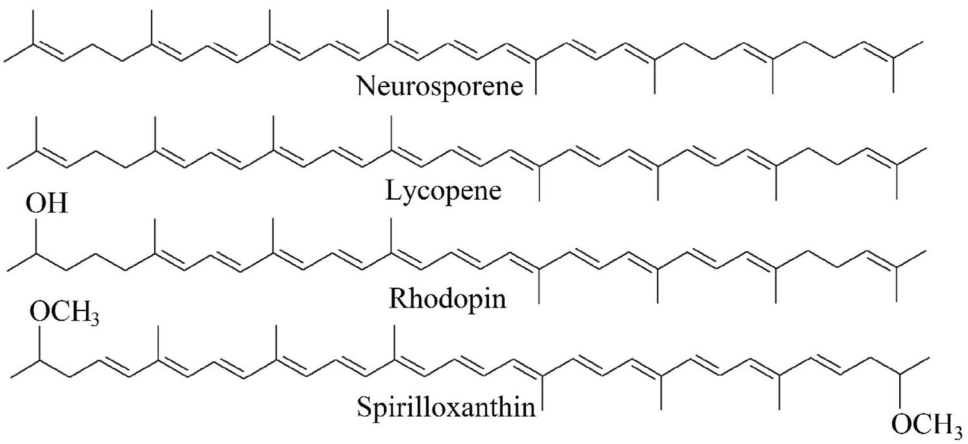

Fig. 1 The structural formulae of the studied carotenoids

Larsen's and Ormerod's media, respectively (see Ashikhmin et al. 2017). Under these conditions, the carotenoids with the short CDB chain were not accumulated in bacterial cells (Ashikhmin et al. 2017). For accumulation of the carotenoids with short CDB chains, inhibitors of carotenoid biosynthesis should be added as was done in our prior papers (Ashikhmin et al. 2020, 2022).

Carotenoid isolation was carried in two stages as described earlier (Ashikhmin et al. 2017, 2022). At the first stage, cells were destroyed by ultrasonic disintegration. A mixture of photosynthetic pigments (carotenoids and bacteriochlorophyll) was extracted from the membranes, and then, carotenoids were extracted from the mixture. In the second stage, individual carotenoids were released by HPLC on the Agilent 1200 (Agilent Technologies, USA) with a preparation column (10 × 250 mm) with a reverse phase of Waters Spherisorb ODS2 (Waters, USA), using the solvent gradient described earlier (Ashikhmin et al. 2017). The purity of isolated carotenoids was additionally checked on an analytical HPLC device Shimadzu (Shimadzu, Japan) using an Agilent Zorbax SB-C18 reverse phase column (4.6 × 250 mm) (Agilent Technologies, USA) at 22 °C. Carotenoids were identified by their absorption spectra and retention time.

A typical HPLC chromatograms of isolated carotenoids are indicated in Supplementary materials. The absorption coefficients of carotenoids were taken from Britton (1995): neurosporene—156; lycopene—185; rhodopin—166 and spirilloxanthin—147 mM^{-1} cm^{-1} (light fraction of petroleum ether).

Singlet oxygen detection

Singlet oxygen was studied in aerated pigment solutions by measuring photosensitized phosphorescence at 1270 nm corresponding to the radiative deactivation of the singlet ($^1\Delta_g$) state of oxygen molecules. Measurements were carried out using the spectrometers described elsewhere (Krasnovsky et al. 2019). The spectrometers allow detection of singlet oxygen phosphorescence under stationary and pulsed LED excitation of photosensitizers. It also makes possible to analyze the spectral parameters (emission and excitation spectra) of phosphorescence and record its kinetics traces after short exciting flashes. To measure excitation spectra, we had a set of five LEDs with the emission maxima at 347, 367, 400, 421, and 460 nm, obtained from the firms Polironic (Russia) and Artleds (Russia). When measuring phosphorescence parameters, the emission power of LEDs on the surface of the cuvette did not exceed 10 mW/cm^2. The half-width of the LED radiation bands was 11–26 nm. For time-resolved measurements, pulsed LEDs equipped with a modulating electronic chips and emission maxima at 365 nm (half bandwidth—18 nm), 395 nm, and 450 nm (half bandwidth—11 nm) (Polironic, Moscow) were used.

LED emission was focused in a spot with a diameter of 5 mm on the surface of a 1 cm quartz cuvette with a tested solution. The average excitation intensity was controlled by the ThorLabs PM-100D power meter with S120VC sensor photovoltaic head (ThorLabs, USA) and Ophir ORION-TH power meter with a 20C-SH thermal sensor head (Ophir Optronics, Israel). Phosphorescence of $^1O_2$ was detected at an angle of 90° relative to the excitation beam using a cooled photomultiplier FEU-112 with the S-1 spectral response (Ekran Optical Systems, Russia) through the cut-off filters that transmit IR emission at the wavelength ≥ 1000 nm, and one of three replaceable interference filters with maximum transmittance at 1230, 1270, and 1310 nm and half-band width of 10 nm. The stationary phosphorescence intensity was recorded using a digital millivoltmeter (Econix-Expert, Russia).

When time-resolved phosphorescence measurements were carried out, the repetition rate and duration of LED pulses were regulated by an external pulse generator. The pulse duration in most measurements was 10 μs, and the pulse repetition frequency was changed in the range of 5–100 Hz. The PMT signal was sent through a broadband (400 MHz) preamplifier to an electronic board operating in a time-resolved photon counting mode (Parsek, Russia). The counting board, which was launched from an additional pulse of the generator synchronized with the LED pulse, divided the time interval between flashes into 256, 512, or 1024 channels. The signal of the board came through the USB port to a personal computer that processed the signal. Kinetic curves were obtained by accumulating PMT impulses in each channel during 2–30 min. The quantum yield of $^1O_2$ generation (Φ_Δ) was measured using as a reference an organic photosensitizer phenalenone (perinaphthenone, 1H_phenalen-1-one) (Merck, USA), which has a broad absorption band with a maximum at 350 nm. It is known that the quantum yield of the $^1O_2$ photogeneration by phenalenone is close to $1(0.95 \pm 0.05)$ (Oliveros et al. 1991; Schmidt et al. 1994). The experiments were carried out using hexafluorobenzene (C_6F_6) as a solvent, which was specially purified for our experiments (Pim-Invest, Russia). This solvent was employed because there are no hydrogen atoms in its molecule. Therefore, the lifetime of singlet oxygen in hexafluorobenzene is very long (16 ms) that facilitates the detection and studies of $^1O_2$. In addition, C_6F_6 does not enter chemical interaction with carotenoids and singlet oxygen (Krasnovsky et al. 2019; Ashikhmin et al. 2020, 2022).

Results

Neurosporene

The absorption spectrum of neurosporene in hexafluorobenzene has three major peaks at 417, 441, and 470 nm (Fig. 2A). Under laser irradiation of neurosporene solutions (2–8 μM), we observed weak phosphorescence at 1270 nm. Excitation spectrum of phosphorescence was estimated using three continuous LEDs with the emission wavelengths of 399, 461, and 530 nm. Details of the measurement procedure were described in previous papers of our group (Ashikhmin et al. 2020, 2022). With each LED, luminescence was detected through three interference filters transmitting light at 1270, 1230, and 1310 nm. Then, at each wavelength, the background luminescence of a quartz cuvette with acetone or 1:1 (v/v) mixture of C_6F_6 and acetone having no carotenoids was recorded. The background signals were subtracted from the signals obtained from carotenoid solutions. The spectral maximum of the resulting difference signals was always observed at 1270 nm that corresponds to the spectral maximum of singlet oxygen phosphorescence.

The main maximum of the phosphorescence excitation spectrum was always observed at 460 nm that corresponds to the main maximum of the neurosporene absorption spectrum (Fig. 3A). Note that the carotenoids with short CDB chains (phytoene, phytofluene, and ζ-carotene) studied in our prior papers have zero absorbance at this wavelength. The long wavelength maxima of these short-chain carotenoids were at 293, 369, and 420 nm, respectively (Ashikhmin et al. 2020, 2022). Therefore, it is excluded that admixture of these carotenoids contributed to the phosphorescence excitation in solutions of neurosporene and other carotenoids investigated in the present work.

The phosphorescence decay time in neurosporene solutions was much shorter than the lifetime of singlet oxygen (τ_Δ) in neat C_6F_6. For detailed analysis, $^1O_2$ phosphorescence was studied in mixed solutions containing both phenalenone and neurosporene. The excitation power was selected so that the degree of the carotenoid destruction during the measurement time did not exceed 5% of the initial absorbance value. Figure 3B indicates that decays of $^1O_2$ phosphorescence arising after excitation of phenalenone by short excitation pulses are exponential. The phosphorescence decay time declined after the addition of neurosporene and the increase of the neurosporene concentration. At the same time, the initial phosphorescence intensity obtained by extrapolating the exponentials to the zero time after the flash [$I_{ph}(0)$] remained unchanged. The latter implies that within the range of the carotenoid concentrations used in our experiments the carotenoid did not influence the rate of the $^1O_2$ generation by phenalenone but they strongly increase the decay rate of singlet oxygen (Fig. 2 B, C).

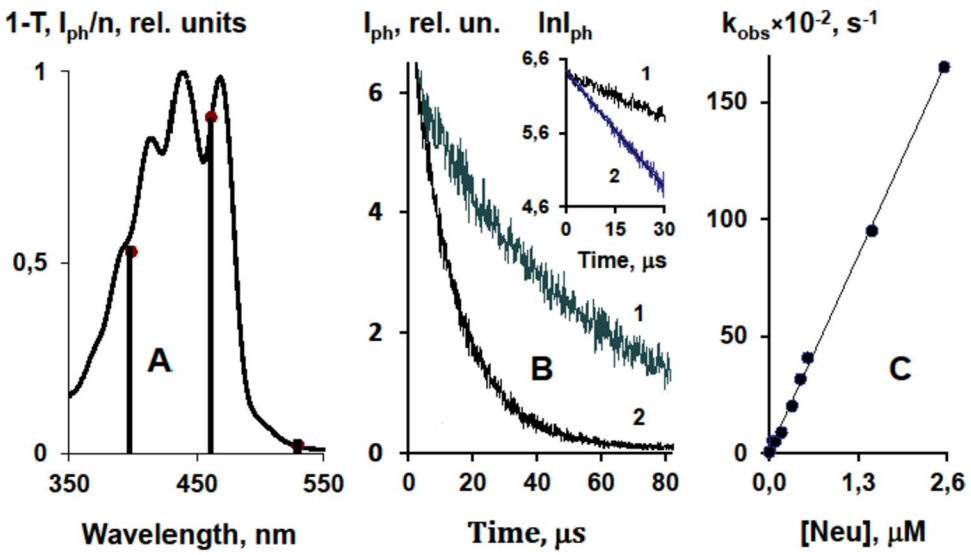

Fig. 2 Neurosporene in C_6F_6. **A** The absorption spectrum of neurosporene (4 μM) (solid line) and the excitation spectrum (vertical lines) of $^1O_2$ phosphorescence at 1270 nm estimated using a set of LEDs (100 mW) with fixed radiation wavelengths, the spectra are normalized at 461 nm (I_{ph} is the phosphorescence intensity in photons per second, n is a number of incident photons), **B** decays of singlet oxygen phosphorescence at 1270 nm photosensitized by phenalenone after LED pulses (2 μs, 405 nm, 1.2 μJ, 10 kHz repetition rate, 10 min accumulation time) in Cartesian or semi-logarithmic coordinates in solutions containing phenalenone (3 μM) and 2.6 (1) and 8.7 (2) μM neurosporene, and **C** the Stern–Volmer plot for the dependence of the phosphorescence decay rates in phenalenone solutions from the concentration of added neurosporene

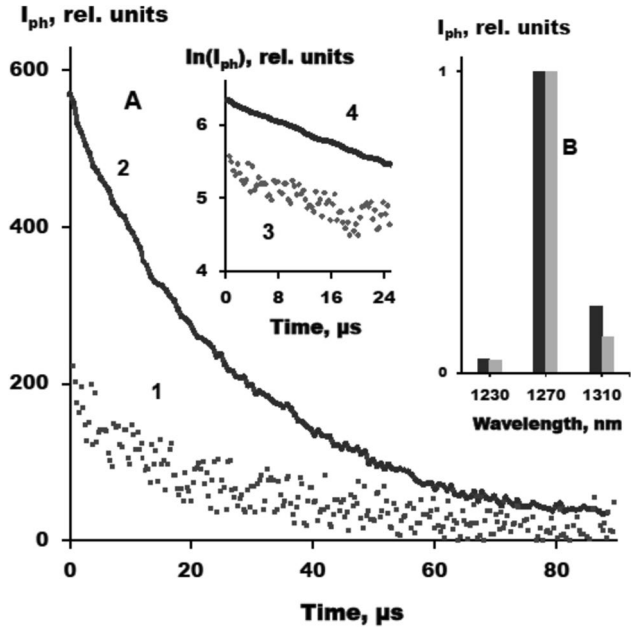

Fig. 3 Determination of the quantum yields of $^1O_2$ photogeneration by carotenoids using lycopene in aerated hexafluorobenzene**. A** Decays of.$^1O_2$ phosphorescence after 10 μs LED pulses (3.6 μJ, 405 nm, 10 kHz repetition rate) in the solution of lycopene (1.8 μM with absorbance of 0.13 at 405 nm) (1, 3) and mixed solution of phenalenone (with absorbance of 0.13 at 405 nm) and lycopene (2, 4) in the Cartesian (1, 2) or semi-logarithmic coordinates (3, 4). The decay curves (2, 4) were reduced 40-fold compared to the original records in order to be seen on the scale of the present figure. The decays were recorded with the 10 μs delay after the start of LED pulses and 40 min accumulation time. **B** Spectra of the phosphorescence emission in solution of lycopene alone (black bars) and in the mixed solution of phenalenone and lycopene (gray bars)

Quenching of $^1O_2$ by neurosporene obeys the Stern–Volmer Eq. (1) (Fig. 1C):

$$k_{obs} = k_o + k_q[Car], \tag{1}$$

where k_{obs} is the observed rate constant of phosphorescence decay (in s^{-1}) after LED pulses in solutions containing both a photosensitizer and Car, k_0 is the rate constant of the phosphorescence decay in phenalenone solutions without Car, and k_q is the bimolecular rate constant of $^1O_2$ quenching by Car. The value of k_q was calculated from the slope of the linear Stern–Volmer plot. The neurosporene concentrations were calculated from the absorbance measurements using the molar absorption coefficient indicated by Britton 1995.

As a result, it was obtained that the neurosporene k_q is rather close to the rate constant of the diffusion- limited reactions (Table 1), being many-fold greater than k_q obtained previously for ς-carotene and phytofluene (Ashikhmin et al. 2022). It is noteworthy that this constant corresponds to a physical quenching process, because under conditions of our experiments, the bleaching of neurosporene was negligible

Table 1 Quantum yields of $^1O_2$ generation (Φ_Δ) and rate constants for $^1O_2$ quenching (k_q) in solutions of carotenoids in hexafluorobenzene obtained in the present and prior (Ashikhmin et al. 2020, 2022) works of our group

Carotenoids	CDB	$\Phi_\Delta \times 10^2$	$k_q \times 10^{10}$ (M^{-1} s^{-1})*
Prior work (Ashikhmin et al. 2020, 2022)			
Phytoene	3	2	0.0004 ± 0.0001
Phytofluene	5	39	0.0036 ± 0.0009
ζ-Carotene	7	1.4	0.021 ± 0.002
This work			
Neurosporene	9	3.0 ± 1.0	0.68 ± 0.08
Lycopene	11	1.5 ± 0.5	1.1 ± 0.08
Rhodopin	11	2.5 ± 0.5	1.0 ± 0.08
Spirilloxanthin	13	≤0.5	1.0 ± 0.08

*Values of k_q were calculated using the molar absorption coefficients (mM^{-1} cm^{-1}) in the main maxima of the carotenoid absorption spectra reported by Britton (1995) (see "Materials and Methods" section)

or was not observed at all. This conclusion agrees with the rates of chemical quenching of singlet oxygen obtained previously in solutions of β-carotene and fucoxanthin (Krasnovsky and Paramonova 1983).

The quantum yields of singlet oxygen were determined using both steady-state and time-resolved phosphorescence measurements. For steady-state measurements, the following basic equation was applied:

$$I_{ph} = I_{ex}\left(1 - 10^{-A}\right)\Phi_\Delta k_r \tau_\Delta, \tag{2}$$

where I_{ph} and I_{ex} are the steady-state intensities (Einstein per second) of phosphorescence and exciting light, respectively. A is absorbance of a photosensitizer at the wavelength of excitation, k_r is the radiative rate constant for $^1O_2$ phosphorescence emission, and τ_Δ is the real lifetime of singlet oxygen in solutions.

As $I_{ph}/(I_{ex}(1 - 10^{-A}))$ is equal to the phosphorescence quantum yield (Φ_{ph}), Eq. 2 can be simplified:

$$\Phi_{ph} = \Phi_\Delta k_r \tau_\Delta. \tag{3}$$

The values of Φ_Δ for carotenoids $(\Phi_\Delta)_{car}$ can be calculated from the ratios of the Φ_Δ values in solutions of carotenoids and phenalenone (Eq. 4). In this case, constants k_r are reduced:

$$\left(\Phi_\Delta\right)_{car} = \left(\Phi_{ph}/\tau_\Delta\right)_{car}/\left(\Phi_{ph}/\tau_\Delta\right)_{phen}. \tag{4}$$

Since carotenoids are very strong quenchers of $^1O_2$, the τ_Δ in carotenoid solutions was about 150-fold smaller than in solutions of phenalenone (16 ms, Krasnovsky et al. 2019).

For time-resolved measurements, another equation was used.

$$I_{ph}(t) = I_{ex}\left(1 - 10^{-A}\right)\Phi_{\Delta}k_r(\exp(-t/t_{\Delta})), \quad (5)$$

where $I_{ph}(t)$ is the instant phosphorescence radiative rates in Einstein per second and I_{ex} is the intensity of short exciting LED pulse in Einstein per pulse. As phosphorescence decays were exponential, extrapolation of the exponential functions to the zero time after exciting pulse is equal to

$$I_{ph}(0) = I_{ex}\left(1 - 10^{-A}\right)\Phi_{\Delta}k_r. \quad (6)$$

This function allows for calculation of $(\Phi_{\Delta})_{car}$:

$$(\Phi_{\Delta})_{car} = \left[I_{ph}(0)/\left(I_{ex}\left(1 - 10^{-A}\right)\right)\right]_{car}/\left[I_{ph}(0)/\left(I_{ex}\left(1 - 10^{-A}\right)\right)\right]_{phen}. \quad (7)$$

Figure 3A illustrates the procedure of the quantum yield measurement using time-resolved detection of singlet oxygen phosphorescence. This procedure was similar for all investigated carotenoids. For illustration, the lycopene solution was chosen.

In the experiment with neurosporene, excitation was produced by 2 µs pulses of LED at 405 nm. The concentration of neurosporene was 2.0 µM. The absorbance of neurosporene at 405 nm was 0.2. In addition, a mixed solution containing both phenalenone and the carotenoid was prepared. The phenalenone concentration was 3 µM. Absorbance at 405 nm was 0.13 in a 1 cm cell. Comparison of the $I_{ph}(0)$ (the zero time phosphorescence intensity) in solutions of phenalenone and neurosporene led us to the value of the quantum yield of $^1O_2$ generation by neurosporene equal to 0.02. Using steady-state measurements, we arrived to the value of 0.04. Average value is indicated in Table 1. Surprisingly, it was slightly higher than that obtained previously for ζ-carotene (Ashikhmin et al. 2022). Nevertheless, due to much stronger quenching of $^1O_2$ by neurosporene, the phosphorescence signal was rather weak. The 3–5-fold smaller signals would be near the noise level and could not be reliably analyzed.

Lycopene

The absorption spectrum of lycopene has three main peaks at 442, 469, and 500 nm (Fig. 4A). The studies were carried out according to the same plan as the studies of neurosporene. Under laser irradiation of lycopene solutions, weak phosphorescence at 1270 nm was observed. Excitation spectrum of phosphorescence was estimated using three continuous LEDs. Figure 4A indicates that the action spectrum correlates with the main maxima of the lycopene absorption spectrum. The phosphorescence decay time in the lycopene-containing solutions decreased with the increase of the lycopene concentration (Fig. 4B). The rate constant of physical quenching of $^1O_2$ by lycopene was calculated from the Stern–Volmer plot of the phosphorescence decay rates versus lycopene concentrations. The obtained k_q was about 2-fold greater than that for neurosporene (Table 1). It is known that lycopene is probably the strongest quencher of

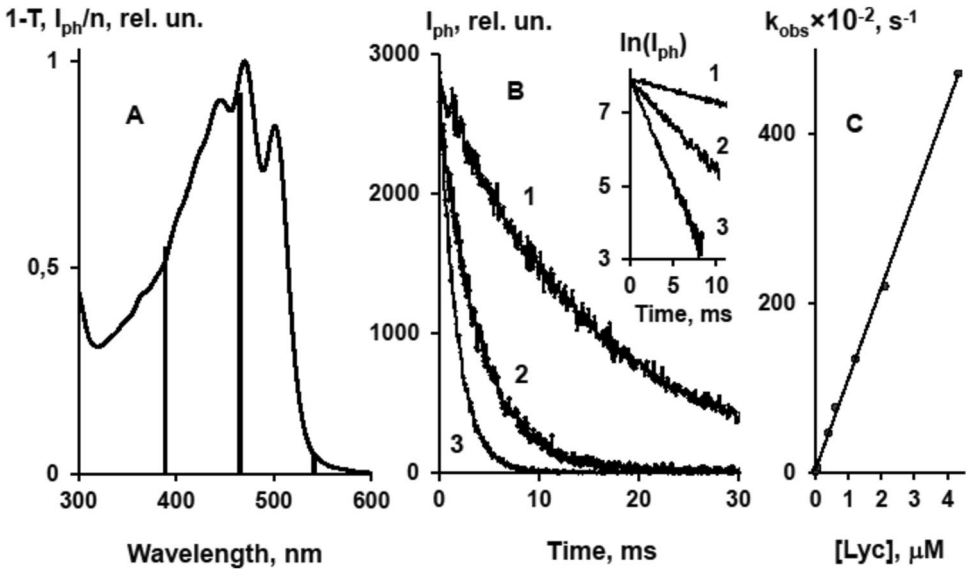

Fig. 4 Lycopene in C_6F_6. **A** The absorption spectrum (solid line) and the excitation spectrum of $^1O_2$ phosphorescence at 1270 nm estimated using a set of LEDs with fixed radiation wavelengths, normalized at 461 nm (vertical lines) (I_{ph} is the phosphorescence intensity in photons per second, n is a number of incident photons), **B** decays of singlet oxygen phosphorescence after LED pulses (10 µs, 405 nm, 6 µJ, 10 Hz repetition rate, 15 min accumulation time) in Cartesian or semi-logarithmic coordinates in solutions containing phenalenone alone (1) and after addition of 0.03 (2) and 0.07 (3) µM rhodopin, and **C** the Stern–Volmer plot for the dependence of the phosphorescence decay rates in phenalenone solutions from the concentration of added lycopene

singlet oxygen among the C_{40} carotenoids with 11 CDB (Di Mascio et al. 1989; Conn et al. 1991). Our data are consistent with this statement, although the difference from other carotenoids is less than that obtained by Di Mascio et al. and resembles the data by Conn et al. (1991).

Figure 3A illustrates the procedure of the quantum yield measurement using time-resolved detection of singlet oxygen phosphorescence in lycopene-containing solutions. Both steady-state and time-resolved methods showed that the quantum yield of $^1O_2$ generation by lycopene is equal to that for ζ-carotene and about 2-fold smaller than in neurosporene solutions, although this difference between the Φ_Δ values for neurosporene and lycopene is close to the measurement error range (Table 1).

Rhodopin

The absorption spectrum of rhodopin has three main peaks at 442, 469, and 496 nm, which are close to the main absorption peaks of lycopene (Fig. 5A). The action spectrum of weak phosphorescence at 1270 nm observed under laser irradiation of rhodopin solutions correlated with the rhodopin absorption spectrum (Fig. 5A). The phosphorescence decay time in rhodopin-containing solutions decreased with the increase of rhodopin concentrations (Fig. 5B). The rate constant of the physical quenching of $^1O_2$ by rhodopin was calculated from the Stern–Volmer plot of the phosphorescence decay rates versus rhodopin concentrations. The k_q obtained was about 10% smaller than that for lycopene (Table 1). The quantum yield of $^1O_2$ photogeneration by rhodopin was estimated from comparison of the $^1O_2$ phosphorescence intensities in the mixed solutions of phenalenone and rhodopin with the same parameters of the solutions of rhodopin alone. For excitation of phenalenone, the LED with the radiation wavelength of 367 nm was used. For excitation of rhodopin, the 460 nm LED was applied. Phenalenone and rhodopin had equal absorbance at the excitation wavelengths. Other experimental conditions were similar to those indicated in Fig. 4, and therefore, the data are not shown. The obtained quantum yield is presented in Table 1.

Spirilloxanthin

The absorption peaks of spirilloxanthin are markedly shifted to longer wavelengths compared to rhodopin. The main absorption maxima are at 462, 490, and 523 nm (Fig. 6). We could not obtain reliable signal of $^1O_2$ phosphorescence in solutions of this pigment. Therefore, it can be proposed that the phosphorescence intensity in solutions of spirilloxanthin is smaller than the sensitivity limit of our spectrometers. It was estimated that the phosphorescence quantum yield is less than 0.5. The rate constants of $^1O_2$ quenching by rhodopin and spirilloxanthin appeared to be very similar.

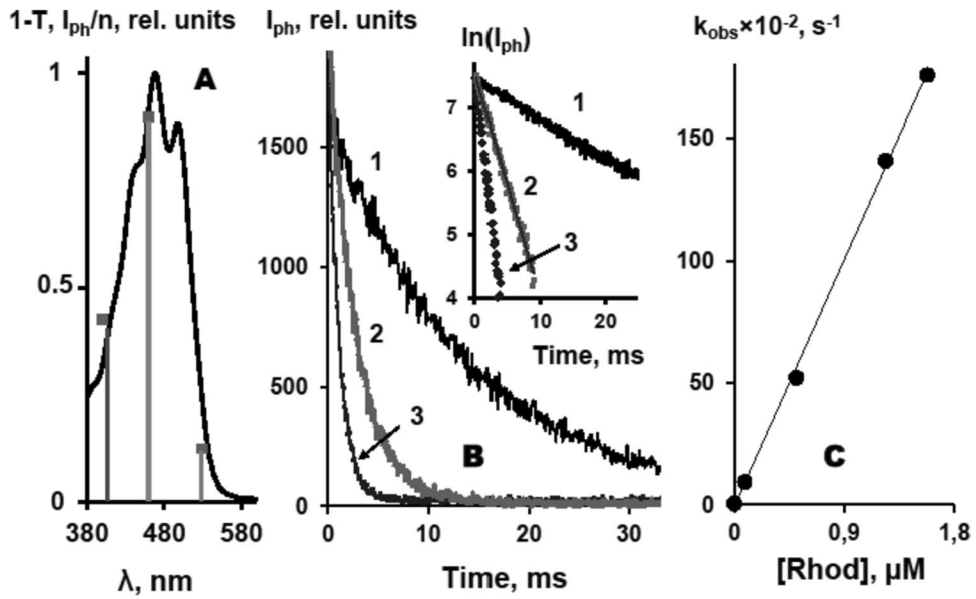

Fig. 5 Rhodopin in C_6F_6. **A** The absorption spectrum (solid line) and the excitation spectrum (vertical lines) of $^1O_2$ phosphorescence estimated using a set of continuous LEDs (100–150 mW) with fixed radiation wavelengths, the spectra are normalized at 461 nm. **B** Decays of singlet oxygen phosphorescence after LED pulses (10 μs, 405 nm, 6 μJ, 10 Hz repetition rate, 15 min accumulation time) in Cartesian or semi-logarithmic coordinates in solutions containing phenalenone alone (1) and after addition of 0.04 (2) and 0.09 (3) μM rhodopin, and **C** the Stern–Volmer plot for the dependence of the phosphorescence decay rates in phenalenone solutions from the concentration of added rhodopin

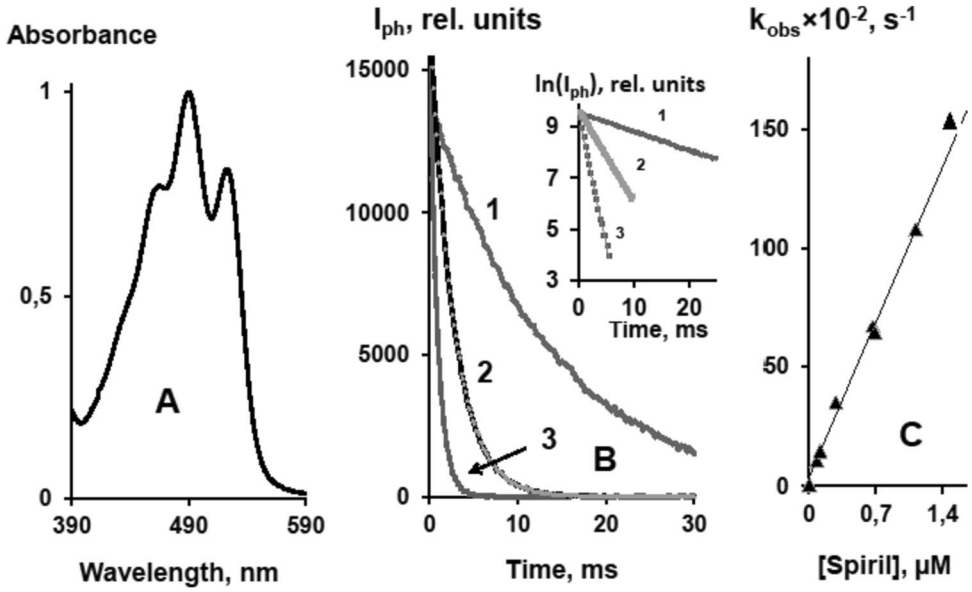

Fig. 6 Spirilloxanthin in C_6F_6. **A** Absorption spectrum of spirilloxanthin, **B** decays of singlet oxygen phosphorescence after LED pulses (10 μs, 405 nm, 6 μJ, 10 Hz repetition rate, 15 min accumulation time) in Cartesian or semi-logarithmic coordinates in solutions containing phenalenone alone (1) and after addition of 0.03 (2) and 0.08 (3) μM spirilloxanthin, and **C** the Stern–Volmer plot for the dependence of the phosphorescence decay rates in phenalenone solutions from the concentrations of added spirilloxanthin

The quenching is physical with the k_q values near the rate constants for the diffusion-limited reactions.

Discussion

Thus, it has been shown for the first time that isolated carotenoid molecules with long chains of CDB (9–11): neurosporene, lycopene, and rhodopin are capable of singlet oxygen generation upon photoexcitation at the wavelength region of their main absorption maxima. The quantum yields were estimated to be $(1.5–3.0)\times10^{-2}$ in solutions of all investigated carotenoids. Photogeneration of singlet oxygen was not observed in spirilloxanthin solutions (Table 1). It was estimated that Φ_Δ in the spirilloxanthin solutions is at least 3-fold smaller than in solutions of lycopene. Comparison with the data of our prior papers (Ashikhmin et al. 2020, 2022) indicates that the carotenoids with long chains of CDB generate $^1O_2$ much less efficiently than phytofluene (5 CDB) and slightly more efficiently than ζ-carotene (7 CDB) (Table 1).

It is known that carotenoids emit fluorescence under photoexcitation (see references in Table 2). A simplified energy diagram of the main electronic transitions in carotenoid molecules is shown in Fig. 7. Major absorption bands correspond to vibronic $S_o(1A_g^-)\rightarrow S_2$ transitions (Frank and Christensen 2008). According to Fujii et al. (2001a, b), the S_2 level is in fact a sum of two levels $1Bu^-$ and $1Bu^+$ (S_2 and S_3). Anyway, for simplicity, sum of these levels is denoted in this paper by one symbol S_2. At longer wavelengths, much weaker symmetry forbidden $S_o(1A_g^-)\rightarrow S_1(2A_g^-)$ transition exists, which is normally not seen in the absorption spectra. Fluorescence is emitted due to radiative deactivation of the S_2 and S_1 states. As indicated in Table 2, an apparent correlation is seen between the Φ_Δ in solutions of phytoene, phytofluene, and ζ-carotene, and the literature values of the quantum yields (Φ_{f1}) and lifetime (τ_{f1}) of the fluorescence corresponding to the forbidden $S_1\rightarrow S_0$ transitions of these carotenoids (see also Ashikhmin et al. 2020, 2022). At the same time, no correlation was observed between Φ_Δ for these carotenoids and fluorescence parameters of the $S_2\rightarrow S_0$ transitions Φ_{f2} and τ_{f2}. The τ_{f2} are very short (of 0.1–0.2 ps) and almost independent of the structure of the investigated carotenoids. The Φ_{f2} values are at least 100-fold smaller than the values of Φ_{f1} (Table 2).

These observations allowed us to propose that the carotenoids with a short chain of CDB generate $^1O_2$ due to energy transfer to oxygen from the T_1 triplet states, which are populated owing to interconversion of the forbidden S_1 state, which in its turn, is formed due to spontaneous deactivation of the S_2 state (Fig. 7) (Ashikhmin et al. 2022). The proposed mechanism agrees with the reported energy and temporal parameters of the triplet states of phytoene, phytofluene, and ζ-carotene (Bensasson et al. 1976).

However, for the carotenoids with 9–13 CDB, there is no correlation between Φ_Δ and literature values of Φ_{f1} and τ_{f1} (Table 2). For instance, Φ_Δ for neurosporene is slightly greater than that for ζ-carotene, whereas the Φ_{f1} and τ_{f1} for neurosporene are much smaller than those for ζ-carotene. Moreover, the yield of neurosporene fluorescence corresponding to the $S_2\rightarrow S_0$ transition (Φ_{f2}) is 2-fold higher than Φ_{f1}, despite the very short lifetime (0.1–0.2 ps) of the $S_2\rightarrow S_0$ fluorescence (Andersson et al. 1995). When number of CDB increases from 5 to 11, Φ_{f2} increases by more than three orders of magnitude, while the Φ_{f1} decreases by more than two orders (Table 2 and refs therein). The both values of

Table 2 Relative quantum yields of $^1O_2$ generation by carotenoids in hexafluorobenzene calculated from the data of Table 1

Carotenoids	CDB	Φ_Δ, rel values	Φ_{f1}, Absolute (relative) values	τ_{f1} (ps)	Φ_{f2}/Φ_{f1}
Phytoene	3	1	0.002[a] (1)	4400[d]	–
Phytofluene	5	20	0.05[a,b] (25)	3000[c]	$\approx 10^{-2}$[b]
ζ-Carotene	7	0.7	0,0014[c] (0.7)	300[c]	$\approx 10^{-1}$[c]
Neurosporene	9	1.5	5.4×10^{-5}[c] (0.027)	21[e]	2–3[c]
Lycopene	11	0,7	4×10^{-6}[c]	4.7[e,f]	≈100[e,f]
Rhodopin	11	1.1	–	4.1[f]	–
Spirilloxanthin	13	≤0.2	–	1.3[e,f,g]	≈100[f]

Comparison with the fluorescence yields and fluorescence lifetimes corresponding to the $S_1 \rightarrow S_0$ and $S_2 \rightarrow S_0$ transitions in carotenoid molecules

[a]Andersson et al. (2001)

[b]Cogdell et al. (1994)

[c]Andersson et al. (1995)

[d]Gavin et al. (1978)

[e]Fujii et al. (2001)

[f]Fujii et al. (2001)

[g]Frank et al. (1997)

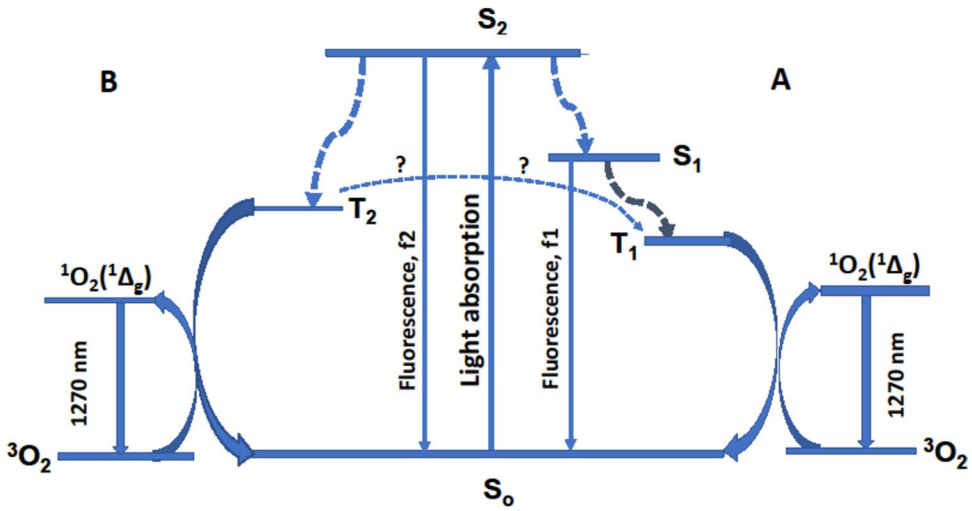

Fig. 7 Tentative energy diagram of the electronic transitions in carotenoid molecules resulting in photosensitization of the $^1O_2$ formation

Φ_Δ and Φ_{f2} are almost the same in the range of carotenoids molecules with 9–11 CDB. It is reasonable to propose based on these observations that singlet oxygen is generated due to the triplets (T_2) formed owing to direct interconversion of the S_2 state without intermediate S_1 population (Fig. 7). To the best of our knowledge, dual triplet state formation has never been observed experimentally (see for instance, Bensasson 1976, Burke et al. 2000). Therefore, it might be suggested that T_2 triplets transfer their energy to oxygen directly with $^1O_2$ formation or populate T_1 due to internal energy transfer from T_2. Further experiments are needed for verification of these assumptions.

Returning to the bacterial complexes of purple bacteria, it is known that rhodopin takes about 90% of the total carotenoid content in the LH2 bacterial cells of *Allochromatium minutissimum* (Britton 2008; Klenina et al. 2022 and refs therein). As Table 1 indicates, the Φ_Δ value in rhodopin solutions is about 100-fold greater than the quantum yield of the $^1O_2$-mediated destruction of BChl in the LH2 complexes of purple bacteria (Klenina et al. 2022).

However, it should be taken into account that BChl strongly quenches singlet oxygen (Krasnovsky 1977, 1979; Krasnovsky et al. 1985; Borland et al. 1987; Egorov et al. 1990). This process is mainly due to a physical mechanism of energy dissipation:

$$^1O_2 + \text{BChl} \rightarrow {}^3O_2 + \text{BChl} + \text{heat}.$$

Contribution of BChl oxygenation is only 3% (Krasnovsky et al. 1985). If it is also true for BChl in bacterial LH2 complexes, we can expect that the quantum yield of rhodopin-photosensitized BChl photodestruction in LH2

complexes should be about 9×10^{-4}. This value reasonably correlates with the data of Klenina et al. (2022). Further studies of this problem are in progress.

The rates constants for $^1O_2$ quenching by carotenoids with 9–13 CDB were found to be close to the rate constants of the diffusion-limited reactions. To our knowledge, the exact values of k_q for phytoene, phytofluene, ζ-carotene, rhodopin, and spirilloxanthin were obtained in our present and prior works (Ashikhmin et al. 2020, 2022) for the first time. Our data support the results of many researchers (Di Mascio et al. 1989; Conn et al. 1991; Foote 1976; Frank and Christensen 2008 and refs therein) that carotenoids with long chain of CDB efficiently deactivate $^1O_2$ due to a physical energy dissipation process**.** It might be that the carotenoids quench $^1O_2$ due to the reverse transfer of energy from singlet oxygen to low-lying triplet levels of carotenoids. Our data do not contradict this hypothesis. However, they are not sufficient for detailed mechanistic analysis of this process.

Thus, our data suggest that the carotenoids with long chain of CDB combine the ability to efficiently deactivate $^1O_2$ with the ability to serve as weak photosensitizers of singlet oxygen generation. Hence, under certain conditions they might play a role of low efficient photosensitizers of photodynamic damage. At the same time, they have a very high potential as protectors of the photosynthetic structures against singlet oxygen attack. However, in the bacterial photosynthetic systems, another potent quencher of singlet oxygen BChl is also present (Krasnovsky 1977; Krasnovsky 1979; Krasnovsky et. al. 1985; Borland et al. 1987; Egorov et al. 1990), due to which the protective function of carotenoids is not so obvious. Similar processes occur also in chloroplasts where both carotenoids and chlorophyll are potent $^1O_2$ quenchers what was discussed many times in the papers of one of us (Krasnovsky 1994 and refs therein).

Supplementary Information The online version contains supplementary material available at https://doi.org/10.1007/s11120-023-01070-6.

Acknowledgements The authors thank Z. A. Zhuravleva (Institute of Basic Biological Problems) for assistance in growing the bacterial cultures used in this study.

Author contributions A. A. Krasnovsky, Jr., A. A. Ashikhmin, A. A. Moskalenko – concept and management of work; A. A. Ashikhmin – extraction of carotenoids; A.S. Benditkis, A. A. Krasnovsky Jr. – design of devices and experimental measurements; A. A. Ashikhmin, A. S. Benditkis, A. A. Moskalenko, A. A. Krasnovsky, Jr. – discussion of the results; A. A. Krasnovsky, Jr., A. A. Ashikhmin, and A. S. Benditkis – writing and editing the text.

Funding This work was carried out with the partial support by the state assignments of the FRC of Biotechnology (12241100080-3) and FRC PSCBR (122041100204-3) of the Russian Academy of Sciences and Russian Science Foundation, Project # 23-65-10005, 2023.

Data availability We do not have formal data availability statement, however, all original experimental data are available upon special request from A.A. Krasnovsky.

Declarations

Conflict of interest The authors declare no conflicts of interest.

Ethical approval This article does not contain description of studies with the involvement of humans or animal subjects.

References

Andersson PO, Bachilo SM, Chen R-L, Gillbro T (1995) Solvent and temperature effects on dual fluorescence in a series of carotenes. Energy gap dependence of the internal conversion rate. J Phys Chem 99:16199–16209. https://doi.org/10.1021/j100044a002

Andersson PO, Takaichi S, Cogdell RJ, Gillbro T (2001) Photophysical characterization of natural *cis*-carotenoids. Photochem Photobiol 74:549. https://doi.org/10.1562/0031-8655(2001)074%3c0549:PCONCC%3e2.0.CO;2

Ashikhmin A, Makhneva Z, Bolshakov M, Moskalenko A (2017) Incorporation of spheroidene and spheroidenone into light-harvesting complexes from purple sulfur bacteria. J Photochem Photobiol B 170:99–107. https://doi.org/10.1016/j.jphotobiol.2017.03.020

Ashikhmin AA, Benditkis AS, Moskalenko AA, Krasnovsky AA Jr (2020) Phytofluene as a highly efficient UVA photosensitizer of singlet oxygen generation. Biochemistry (mosc) 85:773–780. https://doi.org/10.1134/S0006297920070056

Ashikhmin AA, Benditkis AS, Moskalenko AA, Krasnovsky AA Jr (2022) ζ-Carotene: generation and quenching of singlet oxygen, comparison with phytofluene. Biochemistry (mosc) 87:1169–1178. https://doi.org/10.1134/S0006297922100108

Bensasson R, Land EJ, Maudinas B (1976) Triplet states of carotenoids from photosynthetic bacteria studied by nanosecond ultraviolet pulse irradiation. Photochem Photobiol 23:189–193. https://doi.org/10.1111/j.1751-1097.1976.tb07240.x

Borland CF, McGarvey DI, Truscott TJ, Cogdell RG, Land EJ (1987) Photophysical studies of bacteriochlorophyll a and bacteriopheophytin a—singlet oxygen generation. J Photochem Photobiol B 1:93–101

Britton G (1995) UV/visible spectrometry. Carotenoids. In: Britton G, Liaaen-Jensen S, Pfander H (eds) Spectroscopy, vol 1B. Birkhäuser Verlag, Basel

Britton G (2008) Functions of intact carotenoids, in carotenoids. In: Britton G, Liaaen-Jensen S, Pfanger H (eds) Natural functions, vol 4. Birkhauser Verlag, Basel, pp 189–212. https://doi.org/10.1007/978-3-7643-7499-0_10

Burke M, Land EJ, McGarvey DJ, Truscott TG (2000) Carotenoid triplet state lifetimes. J Photochem Photobiol B 59:132–138

Cogdell BJ, Gillbro T, Andersson PO et al (1994) Carotenoids as accessory light-harvesting pigments. Pure Appl Chem 66:1041–1046. https://doi.org/10.1351/pac199466051041

Cogdell RJ, Howard TD, Bittl R et al (2000) How carotenoids protect bacterial photosynthesis. Philos Trans R Soc Lond B 355:1345–1349. https://doi.org/10.1098/rstb.2000.0696

Conn PF, Schalch W, Truscott TG (1991) The singlet oxygen and carotenoid interaction. J Photochem Photobiol B 11:41–47. https://doi.org/10.1016/1011-1344(91)80266-K

Delmelle M (1979) Possible implication of photooxidation reactions in retinal photo-damage. Photochem Photobiol 29:713–716. https://doi.org/10.1111/j.1751-1097.1979.tb07755.x

Di Mascio P, Kaiser S, Sies H (1989) Lycopene as the most efficient biological carotenoid singlet oxygen quencher. Arch Biochem Biophys 274:532–538. https://doi.org/10.1016/0003-9861(89)90467-0

Edge R, Truscott T (2018) Singlet oxygen and free radical reactions of retinoids and carotenoids—a review. Antioxidants 7:5. https://doi.org/10.3390/antiox7010005

Egorov SY, Krasnovsky AA Jr, Vychegzanina IV, Drozdova NN, Krasnovsky AA, (senior), (1990) Photosensitized formation and quenching of singlet molecular oxygen by monomeric and aggregated molecules of the pigments of photosynthetic bacteria. Dokl AN SSSR (biophys) 310:471–476

Foote CS (1976) Photosensitized oxidation and singlet oxygen: consequences in biological systems. In: Pryor WA (ed) Free radicals in Biology, vol 2. Academic, New York, pp 85–133

Frank HA, Christensen RL (2008) Excited electronic states, photochemistry and photophysics of carotenoids. In: Britton G, Liaaen-Jensen S, Pfander H (eds) Carotenoids. Birkhäuser Basel, Basel, pp 167–188

Frank H, Chynwat V, Desamero RZB et al (1997) On the photophysics and photochemical properties of carotenoids and their role as light-harvesting pigments in photosynthesis. Pure Appl Chem 69:2117–2124

Fujii R, Onaka K, Nagae H, Koyama Y, Watanabe Y (2001a) Fluorescence spectroscopy of all-*trans*-lycopene: comparison of the energy and the potential displacements of its $2A_g^-$ state with those of neurosporene and spheroidene. J Lumin 92:213–222. https://doi.org/10.1016/S0022-2313(00)00260-X

Fujii R, Ishikawa T, Koyama Y, Taguchi M, Isobe Y, Nagae H, Watanabe Y (2001b) Fluorescence spectroscopy of all-*trans*-anhydrorhodovibrin and spirilloxanthin: detection of the $1B_u^-$ fluorescence. J Phys Chem A 105:5348–5355. https://doi.org/10.1021/jp010150b

Gavin RM Jr, Weisman C, McVey JK, Rice SA (1978) Spectroscopic properties of polyenes. III. 1, 3, 5, 7-Octatetraene. J Chem Phys 68(2):522–529

Griffiths M, Sistrom WR, Cohen-bazire G, Stanier RY (1955) Function of carotenoids in photosynthesis. Nature 176:1211–1214. https://doi.org/10.1038/1761211a0

Klenina IB, Makhneva ZK, Moskalenko AA, Proskuryakov II (2022) Selective excitation of carotenoids of the *Allochromatium vinosum* light-harvesting LH2 complexes leads to oxidation of bacteriochlorophyll. Biochemistry (mosc) 87:1130–1137. https://doi.org/10.1134/S0006297922100066

Krasnovsky AA Jr (1976) Photosensitized luminescence of singlet oxygen in solution. Biofizika 21:748–749

Krasnovsky AA Jr (1977) Photoluminescence of singlet oxygen in solutions of chlorophylls and pheophytins. Biofizika 22:927–928

Krasnovsky AA Jr (1979) Photoluminescence of singlet oxygen in pigment solutions. Photochem Photobiol 29:29–36. https://doi.org/10.1111/j.1751-1097.1979.tb09255.x

Krasnovsky AA Jr (1994) Singlet molecular oxygen and primary mechanisms of photo-oxidative damage of chloroplasts. Studies based on detection of oxygen and pigment phosphorescence. Proc R Soc Edinb B 102:219–235. https://doi.org/10.1017/S0269727000014147

Krasnovsky AA Jr (2008) Luminescence and photochemical studies of singlet oxygen photonics. J Photochem Photobiol A 196:210–218. https://doi.org/10.1016/j.jphotochem.2007.12.015

Krasnovsky AA Jr, Kagan VE (1979) Photosensitization and quenching of singlet oxygen by pigments and lipids of photoreceptor cells of the retina. FEBS Lett 108:152–154. https://doi.org/10.1016/0014-5793(79)81198-9

Krasnovsky AA Jr, Paramonova LI (1983) Interaction of singlet oxygen with carotenoids: rate constants of physical and chemical quenching. Biofizika 28:725–729

Krasnovsky AA Jr, Vychegzanina I, V., Drozdova, N.N., Krasnovsky, A.A. (senior), (1985) Generation and quenching of singlet molecular oxygen by bacteriochlorophylls and bacteriopheophytins a and b. Dokl AN SSSR (biophys) 283:474–477

Krasnovsky AA Jr, Benditkis AS, Kozlov AS (2019) Kinetic measurements of singlet oxygen phosphorescence in hydrogen-free solvents by time-resolved photon counting. Biochemistry 84:153–163. https://doi.org/10.1134/S0006297919020068

Makhneva ZK, Erokhin YE, Moskalenko AA (2007) Carotenoid-photosensitized oxidation of bacteriochlorophyll dimers in light-harvesting complexes B800–850 in *Allochromatium minutissimum* cells. Dokl Biochem Biophys 416:256–259. https://doi.org/10.1134/S1607672907050080

Makhneva ZK, Bol'shakov MA, Ashikhmin AA, et al (2009) Influence of blue light on the structure stability of antenna complexes from *Allochromatium minutissimum* with different content of carotenoids. Biochem Suppl A 3:123–127. https://doi.org/10.1134/S1990747809020032

Makhneva ZK, Ashikhmin AA, Bolshakov MA, Moskalenko AA (2020) Carotenoids are probably involved in singlet oxygen generation in the membranes of purple photosynthetic bacteria under light irradiation. Microbiology 89:164–173. https://doi.org/10.1134/S0026261720010099

Makhneva ZK, Bolshakov MA, Moskalenko AA (2021) Carotenoids do not protect bacteriochlorophylls in isolated light-harvesting LH2 complexes of photosynthetic bacteria from destructive interactions with singlet oxygen. Molecules 26:5120. https://doi.org/10.3390/molecules26175120

Mathews-Roth MM, Wilson T, Fujimori E, Krinsky NI (1974) Carotenoid chromophore length and protection against photosensitization. Photochem Photobiol 19:217–222. https://doi.org/10.1111/j.1751-1097.1974.tb06501.x

Oliveros EPD, Suardi-Murasecco P, Aminian-Saghafi T et al (1991) 1*H*-phenalen-1-one: photophysical properties and singlet-oxygen production. Helv Chim Acta 74:79–90

Schmidt R, Tanielian C, Dunsbach R, Wolff C (1994) Phenalenone, a universal reference compound for the determination of quantum yields of singlet oxygen $O_2(^1\Delta_g)$ sensitization. J Photochem Photobiol A 79:11–17. https://doi.org/10.1016/1010-6030(93)03746-4

Schweitzer C, Schmidt R (2003) Physical mechanisms of generation and deactivation of singlet oxygen. Chem Rev 103:1685–1758. https://doi.org/10.1021/cr010371d